Polymer Chemistry

Accepted Manuscript

ROYAL SOCIETY OF CHEMISTRY

www.rsc.org/polymers

Polymer Chemistry

RSCPublishing

ARTICLE

Hydrogen peroxide-responsive anticancer hyperbranched polymer micelles for enhanced cell apoptosis

Cite this: DOI: 10.1039/x0xx00000x

Received 00th February 2015,
Accepted 00th February 2015

DOI: 10.1039/x0xx00000x

www.rsc.org/

Bing Liu,[‡a] Dali Wang,[‡b] Yakun Liu,[a] Qian Zhang,[a] Lili Meng,[b] Huirong Chi,[a] Jinna Shi,[c] Guolin Li,*[,a] Jichen Li,*[,a] and Xinyuan Zhu*[,b]

Chemotherapeutic drugs that induce apoptosis in tumor cells via regulating intracellular reactive oxygen species (ROS) levels represent a promising strategy against cancer. Here we reported an effective anticancer nanomicelle system based on hydrogen peroxide (H_2O_2)-responsive hyperbranched polymer through enhancing cell apoptosis for efficient cancer therapy. Firstly, the hydrophobic anticancer drug 7-ethyl-10-hydroxyl-camptothecin (SN38) was conjugated onto a hydrophilic and biocompatible hyperbranched polyglycerol (HPG) via H_2O_2-responsive thioether linkage, forming the SN38-conjugated HPG (HPG-2S-SN38). The amphiphilic HPG-2S-SN38 self-assembled into stable nanomicelles which could encapsulate cinnamaldehyde (CA) that induces apoptotic cell death via ROS production in a large number of cancer cells. The release of SN38 and CA from the CA-loaded HPG-2S-SN38 micelles was dependent on H_2O_2 concentration, whereas CA was released remarkably faster than SN38 under an oxidative condition. The *in vitro* study suggested the CA-loaded HPG-2S-SN38 nanomicelles entered cancer cells rapidly and subsequently were activated by the intracellular oxidative environment to release CA and SN38. The preferentially released CA could effectively induce intracellular ROS production, which in turn accelerated the degradation of micelles and the release of SN38. Compared to the HPG-2S-SN38 micelles and the mixture of CA and SN38, the CA-encapsulated HPG-2S-SN38 micelles resulted in more intracellular ROS generation, which efficiently enhanced the proliferation inhibition of tumor cells via inducing cell apoptosis, exerting a synergistic anticancer effect of CA and SN38. The H_2O_2-sensitive CA-loaded HPG-2S-SN38 micelles that amplified the antitumor effect by enhancing the cell apoptosis have enormous potential as novel anticancer therapeutics.

Introduction

Cancer remains one of the most devastating diseases world-wide and has become the major cause of mortality in many countries.[1] At present, chemotherapy is one of major approaches in clinical treatment.[2,3] Among various chemotherapeutic agents, drugs that are constructed to induce tumor cell apoptosis through ROS generation are an attractive strategy against various malignancies.[4-8] ROS including hydrogen peroxide, hydroxyl radicals and superoxide anion, plays a critical role in cell apoptosis.[9] Generally, high concentration of ROS can damage intracellular components such as lipids, DNA and proteins through inducing biochemical alterations, eventually leading to apoptotic cell death.[10] Up to now, numerous drugs have been developed against cancer by causing apoptosis through ROS-mediated cellular damage.[11-15] Despite their potent anticancer activities, the use of these small-molecular-weight chemotherapeutic drugs or their simple combinations is hampered by their poor water solubility and stability, undesirable side effects, relatively short half-life and lack of specificity toward diseased tissues, which severely reduce their efficiency of arriving at the tumor sites. Furthermore, the simple combination of these chemotherapeutic drugs could not provide a programmable release of various components that may have a better synergistic effect for cancer therapy. As we know, chemotherapy significantly depends on the induction of apoptosis in tumor cells. Therefore, it is still a great challenge to construct highly efficient anticancer therapeutic agents that can improve the tumor specific delivery, release the drugs in a controlled manner and enhance apoptosis selectively in malignant cancer cells.[16,17]

As one kind of emerging materials, hyperbranched polymers have received more and more attention as drug delivery carriers in the past few years because of their unique topological architecture and specific physical/chemical properties.[18-27] They have highly branched and three-dimensional globular architectures, adequate spatial cavities, a large number of terminal functional groups for further conjugation of drug or

targeting/imaging agents and convenient synthetic procedures, which provides an apparent advantage in encapsulating small-molecular-weight drugs.[28-37] Moreover, they can self-assemble into nanomicelles with a relatively low critical micelle concentration.[38] These attractive features provide apparent advantages in biological and biomedical systems and devices, particularly in drug delivery applications. Especially, stimuli-responsive hyperbranched polymers and their assemblies have been widely used as potent biomaterials to construct drug delivery systems because they can release the encapsulated components in a controlled programmable manner.[39-46] Among them, the H_2O_2-sensitive hyperbranched polymeric nanomicelles have drawn increasing attention since the tumor cells have increased level of H_2O_2 up to 0.5 nmol/10^4 cells/h in comparison with normal cells due to the overproduction of ROS.[47-49] Therefore, it is conceivable that if the anticancer drugs are loaded into the H_2O_2-sensitive hyperbranched polymer micelles in different binding forms, a nanodelivery system with tumor-specific delivery and controllable release ability could be easily obtained. Thus, ascribed to the excellent combination of hyperbranched micelles and therapeutic agents related to cell apoptosis, an efficient anticancer chemotherapeutic system with enhanced cell apoptotic death of tumor cells can be expected.

In this work, we constructed H_2O_2-responsive anticancer hyperbranched polymer micelles for co-delivery of the chemotherapeutic drug SN38 and CA for enhancing cell apoptosis through ROS generation. The SN38 was conjugated onto HPG through H_2O_2-sensitive thioether bonds to form amphiphilic hyperbranched polymer HPG-2S-SN38, which could further self-assemble into nanomicells. Then the other anticancer drug CA was loaded into the HPG-2S-SN38 micelles due to the physical interaction. The disruption of CA-loaded HPG-2S-SN38 nanomicelles under an exclusive oxidative microenvironment within cancer cells would lead to a faster release of the CA due to the physical encapsulation, resulting in improved ROS generation in tumor cells. The improved ROS levels accelerated the disassembly of the HPG-2S-SN38 micelles and improved the release of CA and SN38, which efficiently enhanced the cytotoxicity of anticancer drugs by activation of apoptotic pathways. Here *in vitro* anticancer evaluation demonstrated that CA-loaded HPG-2S-SN38 micelles exhibited a superior anticancer efficacy when compared with HPG-2S-SN38 micelles and the physical mixture of CA and SN38.

Experimental Section

Apparatus

Nuclear magnetic resonance (NMR) spectroscopy (Mercury plus 400 spectrometer 400 MHz, Varian, U.S.A.) was used with dimethyl sulfoxide-d_6 (DMSO-d_6) or deuterated chloroform ($CDCl_3$) as solvents. The number-average molecular weight (Mn) and weight-average molecular weight (Mw) of the synthesized polymers were determined by gel permeation chromatography (GPC) measurement which was performed on a Perkin-Elmer series 200 system (10 μm PL gel 300 × 7.5 mm mixed-B and mixed-C column, linear polystyrene calibration) equipped with refractive index (RI) detector and used DMF containing 0.01 M lithium bromide as the mobile phase at a flow rate of 1.0 mL/min at 70 °C. Differential scanning calorimeter (DSC) was carried out on a Perkin-Elmer Pyris 1 under a pure nitrogen atmosphere using indium to calibrate temperature and enthalpy. Samples were first heated from room temperature to 50 °C, held at this temperature for 3 min to eliminate the thermal history, and then cooled to -80 °C. Thereafter, these samples were heated again at a rate of 10 °C/min to 50 °C. Transmission electron microscopy (TEM, JEM-2010HT) studies were carried out to investigate the shape and size of micelles. Samples were prepared by directly dropping the micelle solution (0.5 mg/mL) onto a carbon-coated copper grid and then air-drying at room temperature overnight prior to observation. Dynamic light scattering (DLS) measurements were recorded using a Malvern Zetasizer Nano S apparatus equipped with a 4.0 mW laser operating at λ = 633 nm. All samples of 0.5 mg/mL were tested with a scattering angle of 173° at 25 °C. The UV-vis spectra of all samples were recorded on a Perkin-Elmer Lambda 20/2.0 UV-vis spectrophotometer.

Materials

Glycerol (97%, Aldrich), acryloyl chloride (98%, Adamas), 1,2-ethanedithiol (98%, Adamas), methacrylic anhydride (94%, Adamas), 7-ethyl-10-hydroxycamptothecin (98%, TCI) and cinnamaldehyde (99%, Adamas) were used as received. *N*,*N*-dimethylformamide (DMF), methylene dichloride (CH_2Cl_2), BF_3•Et_2O, dimethylsulfoxide (DMSO) and triethylamine (Et_3N) were dried over calcium hydride and then distilled before use. Pyridine (anhydrous, 99.5+%) was obtained from Alfa and used as received. Dulbecco's modified eagle's medium (DMEM) and fetal bovine serum (FBS) were purchased from Sigma and used as received. The Annexin V-FITC/PI apoptosis detection kit was obtained from Invitrogen. 3-(4,5-Dimethyl-thiazol-2-yl)-2,5-diphenyl tetrazolium bromide (MTT) was purchased from Sigma. Dialysis tubes were purchased from Shanghai Lvniao Technology Corp. Clear polystyrene tissue culture treated 6-well, 12-well and 96-well plates were obtained from SangonBiotech (Shanghai, China). Dialysis tube was purchased from Shanghai Lvniao Technology Corp.

Synthesis of HPG

HPG was prepared by the cationic polymerization of glycidol as previously described.[50] Polymerization was carried out in a 500 mL three-necked round-bottomed flask equipped with a magnetic stirrer, a thermometer and a tap funnel under argon atmosphere. Initially, a solution of BF_3•Et_2O (5.35 g, 37.7 mmol) in CH_2Cl_2 (250 mL) was added into the flask. Then, 25 mL of glycidol (372 mmol) was added dropwise over a period of 2 h using the tap funnel at a temperature of -20 ± 5 ^oC. After completed, the mixture was stirred for an additional 24 h. The polymerization was quenched with deionized water and the resulting solution was evaporated under reduced pressure to remove the CH_2Cl_2. After that, the crude product was dissolved in 80 mL of deionized water and precipitated in THF for three times to afford 15.86 g of transparent and highly viscous liquid with a yield of 70%.

Synthesis of HPG-2S-SN38

SN38 (1.0 g, 2.55 mmol) and methacrylic anhydride (1 mL, 6.50 mmol) were simultaneously dissolved in a mixed solvent of pyridine (20 mL) and DMF (30 mL) and then stirred overnight at 40 ^oC. After evaporating under reduced pressure to remove the solvents, the residue was redissolved in chloroform and then precipitated in hexane. The precipitate was isolated and washed with hexane for three times. After dried under vacuum, compound 1 (1.1 g, yield 94%) was obtained. ^{1}H-NMR (400 MHz, $CDCl_3$, δ): 8.24-8.27 (d, 1H), 7.85 (s, 1H), 7.68 (s, 1H), 7.56-7.59 (d, 1H), 6.45 (s, 1H), 5.85 (s, 1H), 5.71-

5.75 (d, 1H), 5.26-5.31 (t, 3H), 3.85 (s, br, 1H), 3.11-3.18 (q, 2H)，2.12 (s, 3H), 1.84-1.95 (m, 2H), 1.38-1.42 (t, 3H), 1.00-1.04 (t, 3H).

1.3 g (17 mmol of -OH groups) of HPG in 20 mL of dry DMF containing 0.23 mL (1.7 mmol) of Et_3N was cooled in an ice-water bath with stirring. After stirring for 30 min, acryloyl chloride (0.14 mL, 1.7 mmol) in 10 mL of anhydrous DMF was added dropwise to the reaction mixture and stirred for an additional 24 h at ambient temperature. After filtration, DMF was removed by vacuum and the residual mixture was redissolved in DMSO. The resulting mixture was dialyzed (MWCO = 1 kDa) against DMSO for 12 h and deionized water for another 24 h (Note: exchanged deionized water at appropriate intervals) and followed by freeze-drying to obtain the pure product 2.

1,2-Ethanedithiol (2 g, 21 mmol) and 0.2 mL Et_3N were dissolved in 10 mL of dry DMF. Then 1.0 g of above esterified HPG in 20 mL of dry DMF was added dropwise using the tap funnel. After that, the mixture was stirred overnight at room temperature and purified by dialyzing (MWCO = 1 kDa) against DMSO for 24 h (Note: exchanged DMSO at appropriate intervals). DMF was removed by vacuum to obtain the pure product 3.

Compound 1 (0.17 g), compound 3 (0.56 g) and 0.05 mL of Et_3N were dissolved in 10 mL of DMSO, and stirred overnight at room temperature. The crude product was purified by dialyzing (MWCO = 1 kDa) against DMSO for 24 h and then reduced under vacuum to evaporate the DMF to obtain the pure HPG-2S-SN38 (0.25 g, yield 34%).

Preparation of HPG-2S-SN38 micelles

Briefly, 8 mg HPG-2S-SN38 was added into 2 mL of DMSO and the mixture was kept stirring at room temperature for 2 h. Then, the solution was added dropwise into 8 mL of deionized water and kept stirring for 1 h. Then, the resulting solution was transferred into a dialysis bag (MWCO = 3.5 kDa) and dialyzed in deionized water for 24 h, during which the deionized water was replaced with fresh one every 4 h. The appearance of turbidity in the aqueous solution suggested the formation of aggregation.

Determination of critical micelle concentration (CMC)

A known amount of 1,6-diphenyl-1,3,5-hexatriene (DPH) solution was added to a series of vials with HPG-2S-SN38 solution to give a final concentration of 5.0×10^{-6} M. The solutions were stirred overnight in dark. The absorbance spectra of all solutions were recorded using Perkin-Elmer Lambda 20/2.0 UV-vis spectrometer. The CMC value was obtained as the intersection of the tangents to the two linear portions of the graph of the absorbance intensity at 313 nm as a function of HPG-2S-SN38 concentration.

Preparation of CA-loaded HPG-2S-SN38 micelles

HPG-2S-SN38 (8.0 mg) and a predetermined amount of CA were simultaneously dissolved in DMSO and stirred at room temperature until completely dissolved. After that, 8 × volumes of deionized water were slowly added into the above solution while stirring and the resulting mixture was kept stirring for 12 h at room temperature. Finally, the mixture was purified by dialysis (MWCO = 3.5 kDa) for 24 h.

To determine the drug loading content (DLC) and drug loading efficiency (DLE), the CA-loaded HPG-2S-SN38 micelle solution after dialysis was lyophilized and redissolved in DMSO. The concentration of SN38 and CA were determined by measuring their UV absorbances by UV-vis spectrophotometer (Perkin-Elmer Lambda 20/2.0 UV-vis spectrometer) and then comparing them with their calibration curves in DMSO. Finally, DLC and DLE of CA-loaded HPG-2S-SN38 micelles were calculated by using the following equations:

DLC (wt%) = (weight of loaded drug/weight of polymer) × 100%

DLE (%) = (weight of loaded drug/weight of drug in feed) × 100%

Release kinetics of SN38 and CA from HPG-2S-SN38 micelles

A total of 3 mL of CA-loaded HPG-2S-SN38 micelles was transferred to a dialysis bag (MWCO = 3.5 KD). It was immersed in 40 mL of phosphate buffer (pH 7.4) or phosphate buffer (pH 7.4) with different concentrations of H_2O_2 solutions in a shaking water bath at 37 ^{o}C. 2 mL of the solution was withdrawn and replaced with an equal volume of fresh media at predetermined time intervals. The amount of SN38 and CA released from micelles was determined with UV measurement.

Cell culture

MCF-7 cells (breast adenocarcinoma), HN-4 cells (oral squamous carcinoma) and HeLa cells (human uterine cervix carcinoma) were all cultivated in DMEM supplied with 10% FBS and antibiotics (50 units/mL penicillin and 50 units/mL streptomycin) at 37 °C in a humidified atmosphere containing 5% CO_2.

Cellular uptake of CA-loaded HPG-2S-SN38 micelles

The experiments of cellular uptake were carried out on flow cytometry and fluorescence microscopy. In order to evaluate the internalization efficacy of CA-loaded HPG-2S-SN38 micelles by tumor cells, nile red (NR) was encapsulated into the micelles instead of CA as a fluoresence probe.

For flow cytometry, MCF-7 cells were seeded in six-well plates at a density of 5×10^5 cells per well with 2 mL DMEM containing 10% FBS and allowed to attach at 37 °C for 24 h. Then, the NR-loaded HPG-2S-SN38 micelles dissolved in DMEM culture medium were added into different wells and the cells after treatment were further incubated at 37 °C for 0.25, 0.5, 1, 2 and 4 h, respectively. After incubation, the cells were rinsed with PBS, treated with trypsin and prepared for flow cytometry analysis. Data for 1.0×10^4 gated events were collected and analyzed using a BD FACSCalibur flow cytometer and Cell Quest software.

For the fluorescence microscopy studies, MCF-7 cells were seeded in twelve-well plates at a density of 2×10^5 cells per well in 1 mL of complete DMEM and cultured for 24 h. Then, the medium was carefully replaced with fresh DMEM culture medium containing NR-loaded HPG-2S-SN38 micelles, and the cells were further incubated at 37 °C for 0.25, 0.5, 1, 2 and 4 h, respectively. After that, the cells were washed with cold PBS for three times and fixed with 4% paraformaldehyde for 30 min at room temperature. Thereafter, the cells were rinsed with cold PBS for another three times and stained with Hoechst33342 for 10 min. Finally, the slides were mounted and directly observed under a fluorescence microscope (Leica DMI6000 B) and a confocal laser scanning microscopy (Nikon A1Si).

***In vitro* cytotoxicity studies**

The cytotoxic effects of different drug formulations were evaluated by the MTT assay. MCF-7, HN-4 cells or HeLa cells

were plated in 96-well plates at a density of 1.0×10^4 cells per well in 200 μL of medium. The culture medium was carefully removed after incubation for 24 h and replaced with 200 μL of medium containing serial dilutions of SN38, CA, HPG-SN38 micelles, CA-loaded HPG-SN38 micelles or mixture of SN38 and CA. After incubation for predetermined time intervals at 37 °C, 20 μL of MTT assays stock solution (5 mg/mL) was added into each well. After incubating for another 4 h, the medium containing unreacted dye was removed carefully and 200 μL of DMSO was then added per well to dissolve the obtained blue formazan crystals. The absorbance was determined in a BioTek® Synergy H4 at a wavelength of 490 nm.

Apoptosis analyses

MCF-7 cells were incubated with SN38, CA, HPG-SN38 micelles, CA-loaded HPG-SN38 micelles or mixture of SN38 and CA at the same doses of SN38 or (and) CA for 24 h. Thereafter, both floating and attached cells were collected, washed three times with PBS, and incubated at room temperature for 15 min with Annexin V-FITC and propodium iodide (PI). All the samples were analyzed with a BD LSR Fortessa flow cytometer.

Determination of intracellular ROS levels

The levels of ROS generated in MCF-7 cells treated with CA, SN38, HPG-2S-SN38 micelles, physical mixture of SN38 and CA, or CA-loaded HPG-2S-SN38 micelles were determined by a fluorometric assay using 2',7'-dichlorfluorescein-diacetate (DCFH-DA) as a fluorescence probe. Once DCFH-DA entered the cells, it would react with intracellular ROS to produce a fluorescent compound dichloroflurescein (DCF).

For the fluorescent microscopy studies, MCF-7 cells were plated in six-well plates at a density of 2×10^5 cells per well in 2 mL of complete DMEM and cultured for 24 h, followed by removing culture medium and adding the above five drug formulations in 2 mL of medium at equivalent doses of CA (20 μg/mL) or (and) SN38 (10 μg/mL). After incubation for 24 h, the cells were washed with PBS twice and then treated with DCFH-DA for 30 min. After that, cells were washed with PBS again and fixed with 4% paraformaldehyde for 30 min at room temperature. Finally, the slides were rinsed with PBS for three times, mounted and directly observed under a fluorescence microscope.

For the relative quantification of intracellular ROS generation, MCF-7 cells were plated in 96-well plates at a density of 1×10^4 cells per well in 200 μL of complete DMEM. After cultivation for 24 h, the cells were exposed to different drug formulations at the same SN38 (10 μg/mL) or (and) CA (20 μg/mL) concentrations for 24 h, washed with PBS, and then incubated with 30 μM DCFH-DA at 37 °C for 30 min. Finally, all the cells were washed with PBS again and fluorescence data was measured in a BioTek® Synergy H4 using an excitation wavelength at 488 nm and an emission wavelength at 525 nm.

Caspase-3 activity analysis

MCF-7 cells were treated by the same procedures as those in the ROS level analysis. Caspase-3 activity was determined by using the caspase colorimetric protease assay kit (Keygen Biotech, Nanjing, China) following the manufacturer's instructions. The optical density was measure at 405 nm. The obtained value of the cells without any treatment was set as 100%.

Statistical analysis

Data are presented as the mean ± standard deviation (SD) from three independent experiments. Statistical significance was examined using Student's t-test for comparing paired sample sets. A p value of < 0.05 was considered statistically significant.

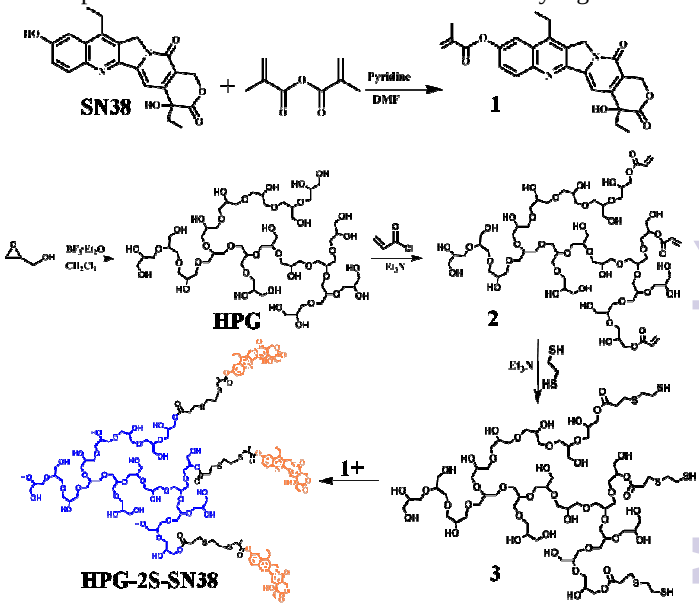

Scheme 1. Synthesis route of H_2O_2-responsive hyperbranched polymer HPG-2S-SN38.

Results and discussion

Synthesis and Characterization of HPG-2S-SN38

The hyperbranched and functional HPG-2S-SN38 was synthesized in several steps starting from glycidol, as displayed in Scheme 1. Firstly the transparent, highly viscous and yellowish HPG was synthesized by the cationic polymerization of glycidol. The ^{1}H NMR spectrum of HPG has been given in the Supplementary Information (Figure S1). The detailed characterization data of HPG can also refer to our previous publication.[50] Subsequently, the HPG was reacted with acryloyl chloride to introduce the terminal acryloyl groups on HPG. The structure of acryloyl-terminated HPG was confirmed by ^{1}H NMR in the Supplementary Information (Figure S2). Next, the acryloyl-terminated HPG was reacted with an excess of 1,2-ethanedithiol in the presence of Et_3N to afford the thiol-terminated HPG. Finally, the thiol-terminated HPG was reacted with SN38 derivative in DMSO to give HPG-2S-SN38. The obtained HPG-2S-SN38 was firstly characterized by ^{1}H NMR. Typical ^{1}H NMR spectrum of HPG-2S-SN38 is displayed in Figure 1. Then the molecular weights and polydispersities of HPG and HPG-2S-SN38 were determined by GPC. Figure 2 gives the GPC curves of HPG and HPG-2S-SN38. The corresponding GPC data have been summarized in Table 1. Additionally, one thermal transition at -68.3 °C is found in the DSC curve of HPG, which can be ascribed to its glass transition (Figure S3). However, there is no thermal transition for the functional HPG-2S-SN38.

HPG is one important type of hyperbranched polyethers with good biocompatibility.[20,21,28-32] It combines high stability, good solubility and low/absent immunogenicity. Up to now, HPG and its derivatives have shown great potential in a variety of biomedical applications such as diagnostics and therapy.[20] In particular, HPG is very suitable as an ideal carrier for various hydrophobic drugs because of their highly hydrophilic nature

and numerous functional groups. The anticancer drug SN38 has been reported to be an inhibitor of DNA topoisomerase I, which can induce ROS generation in cells.[51,52] It exhibits 100- to 1000-fold higher cytotoxicity against many cancer cells *in vitro* in comparison with clinical cancer chemotherapy drug irinotecan hydrochloride which is a hydrosoluble prodrug of SN-38.[52] However, the therapeutic efficacy of SN38 is limited by its low solubility and pharmaceutically acceptable excipients.[53] In this work, SN38 was chemically conjugated with terminals of HPG via thioether linkages to form H_2O_2-responsive drug-conjugated hyperbranched polymers. The thioether bond is very sensitive to H_2O_2 and easily hydrolyzes under oxidative conditions, thus releasing free SN38.[52,54] The content of SN38 moiety in HPG-2S-SN38 is about 5.6 wt%, which is determined by UV-vis spectrophotometer.

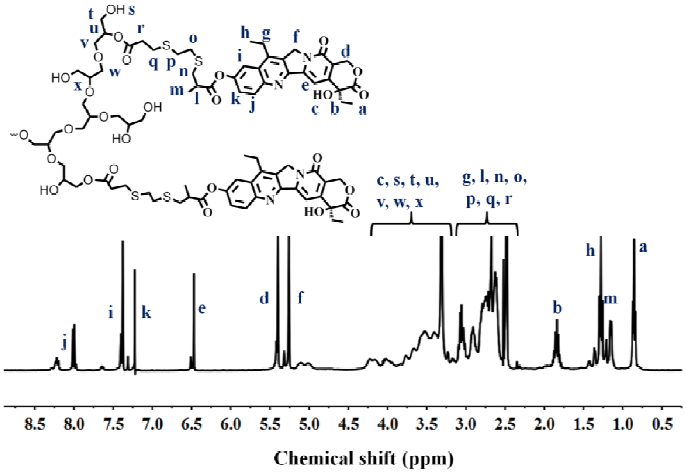

Figure 1. ^{1}H NMR spectrum of HPG-2S-SN38 (400 MHz, DMSO-d_6).

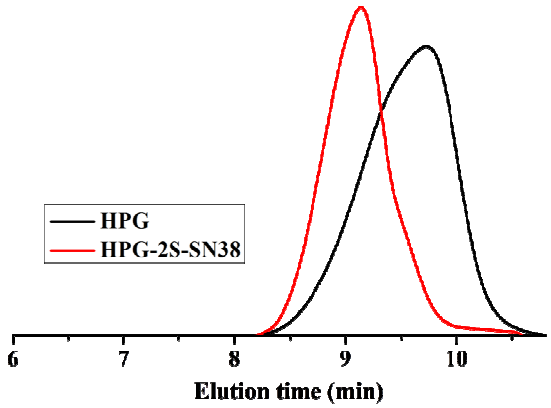

Figure 2. GPC curves of hyperbranched polymer HPG and drug conjugated HPG-2S-SN38.

Table 1. The molecular weights and polydispersities of HPG and HPG-2S-SN38.

Polymers	M_n	M_w	M_w/M_n
	(g/mol; × 10^3)	(g/mol; × 10^3)	
HPG	4.1	9.5	2.3
HPG-2S-SN38	5.4	10.0	1.8

Determined by gel permeation chromatography (GPC) using DMF as the eluent.

Fabrication of HPG-2S-SN38 micelles and CA-loaded HPG-2S-SN38 micelles

Benefiting from its amphiphilic nature, the hyperbranched polymer HPG-2S-SN38 could self-assemble into nanoscale micelles possessing hydrophobic SN38 core and hydrophilic HPG shell in aqueous solution. Firstly, the formation of hyperbranched polymer nanomicelles was confirmed by UV-vis technique. The DPH was used as a probe.[55,56] Figure 3 shows the relationship of the intensity of DPH absorbance versus the polymer HPG-2S-SN38 concentration. The absorbance intensity keeps almost constant at low polymer concentration whereas increases sharply when the polymer concentration reaches a value, indicating that the hydrophobic DPH molecules are transferred from the water environment to the hydrophobic micellar core. It confirms the formation of hyperbranched polymer micelles. This hyperbranched polymer has a relatively low CMC (0.00641 mg/mL), suggesting the high stability of HPG-2S-SN38 micelles. The relatively low CMC value can mainly be ascribed to the strong hydrophobic SN38 and the linkers between SN38 and HPG.

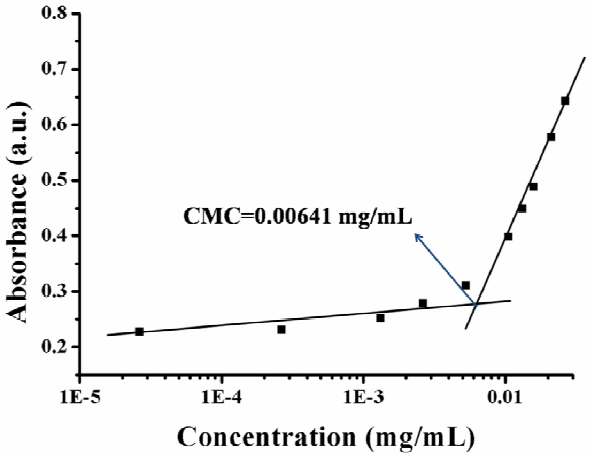

Figure 3. CMC of drug conjugated hyperbranched polymer HPG-2S-SN38.

Moreover, the size of HPG-2S-SN38 micelles was evaluated by DLS. The DLS plot reveals an average hydrodynamic diameter of 54 nm (Figure 4A). TEM measurement was further taken to assess the size and morphology of HPG-2S-SN38 micelles. As displayed in Figure 4B, approximately spherical micelles with an average diameter of 41 nm are observed.

Cinnamaldehyde (CA), an active compound isolated from cinnamomum cassia, is known to possess marked antitumor effects in treating different kinds of solid malignant tumors.[57] A number of studies have demonstrated that CA induces apoptotic cell death via ROS generation, ROS-mediated mitochondrial permeability transition and caspase activation, thereby inhibiting tumor cell proliferation.[58] Despite its potent anticancer activities, the usage of CA in clinical application is hampered by its limited water solubility, relatively short half-life and lack of specificity toward tumor sites.[57,59] Here the hydrophobic anticancer drug CA was loaded into the core of the HPG-2S-SN38 micelles in order to overcome the aforementioned limitations and improve the anticancer efficacy of CA (Scheme 2). The DLE and DLC of the CA-loaded HPG-2S-SN38 micelles are 11.25% and 22.5%, respectively, when the feed ratio of HPG-2S-SN38 to CA is chosen to be 2:1. It should be noted that after loading of CA, HPG-2S-SN38

micelles have larger sizes of ca. 60 nm, which is calculated according to the TEM photograph in Figures 4D and S4. The increase of CA-loaded HPG-2S-SN38 micelle size is also revealed by DLS technique. The DLS result shows that the size of the CA-loaded HPG-2S-SN38 micelles is 75 nm and the size distribution is 0.18 (Figure 4C).

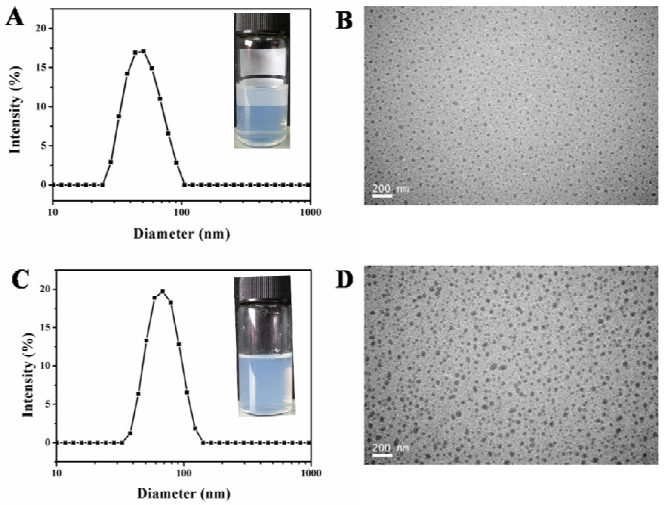

Figure 4. (A) The DLS result of HPG-2S-SN38 micelles. (B) The TEM photograph of HPG-2S-SN38 micelles. (C) The DLS result of the CA-loaded HPG-2S-SN38 micelles. (D) The TEM photograph of the CA-loaded HPG-2S-SN38 micelles.

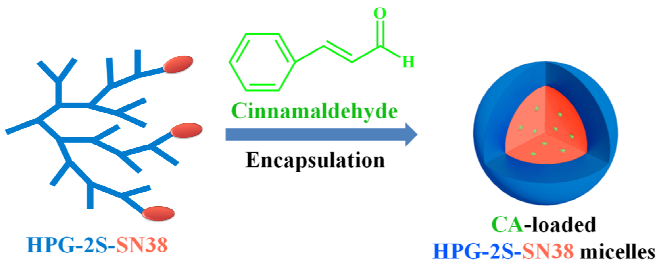

Scheme 2. Construction of the CA-loaded HPG-2S-SN38 micelles.

H_2O_2-triggered destabilization of HPG-2S-SN38 micelles

Thioether groups between SN38 and HPG are hydrophobic at physical conditions but can easily become hydrophilic sulfone or sulfoxide after oxidation, subsequently triggering a quick hydrolysis of the phenol ester and release of SN38.[52] To demonstrate H_2O_2-triggered destabilization of micelles, DLS measurement was taken to monitor the size change of HPG-2S-SN38 micelles treated with 1 mM H_2O_2 in PBS buffer (pH 7.4, 50 mM). Remarkably, HPG-2S-SN38 micelles show fast aggregation, in which micelle size increases from 75 nm to 675 nm after 4 h, and reaches over 1000 nm in 24 h (Figure 5A). The increase of the micelle size may be due to the aggregation of partly dissociated fragments of HPG-2S-SN38. In contrast, the micelle size remains unchanged after 24 h in the absence of H_2O_2 under otherwise the same conditions. These results demonstrated that HPG-2S-SN38 micelles are sensitive to H_2O_2 and could be destroyed under the oxidative condition. In order to further confirm whether the HPG-2S-SN38 is converted into free SN38 after oxidization, the molecular weight of the components after oxidation was determined by ultra performance liquid chromatography & triple quadrupole mass spectrometer (UPLC-3QMS). Figures S5 and S6 give the retention time and the molecular weight. This result indicates that the oxidation of the thioether bond causes a quick hydrolysis of the phenol ester and then leads to fast drug release. As analyzed by UPLC-3QMS, the released drug was found to be the parent SN38.

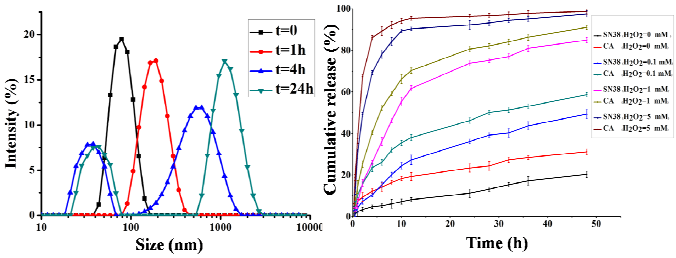

Figure 5. (A) The size change of HPG-2S-SN38 micelles in response to 1 mM H_2O_2 in PBS buffer (pH = 7.4) measured by DLS. (B) Oxidation-triggered release of CA and SN38 from the CA-loaded HPG-2S-SN38 micelles (pH 7.4, 50 mM) at 37 °C.

In vitro CA and SN38 release from CA-loaded HPG-2S-SN38 micelles

The *in vitro* release behavior of the CA-loaded HPG-2S-SN38 micelles was evaluated in pH 7.4 PBS buffer at 37 °C in the presence or absence of H_2O_2. The drug release curves of SN38 and CA from the CA-loaded HPG-2S-SN38 micelles at various H_2O_2 concentrations have been presented in Figure 5B. Remarkably, the results show that CA-loaded HPG-2S-SN38 micelles release CA and SN38 rapidly in the presence of H_2O_2, an oxidative environment similar to that of the intracellular compartments such as cytoplasm and nucleus. For instance, ca. 70% CA and 60% SN38 are released in 12 h in the present of 1 mM H_2O_2. As a contrast, minimal drug release (SN38<20%, CA<30%) is observed even after 48 h incubation under the same conditions in the absence of H_2O_2. These results indicate that the CA-loaded HPG-2S-SN38 micelles are stable in physiological condition but easily cleavable under the oxidative conditions because of the redox-triggered cleavage of thioether linkages. It should be noted that the loaded CA is released faster than the conjugated SN38 under the oxidation conditions. It can be expected that the cleavage of SN38 covalent linkages is slower than the physical release of CA.

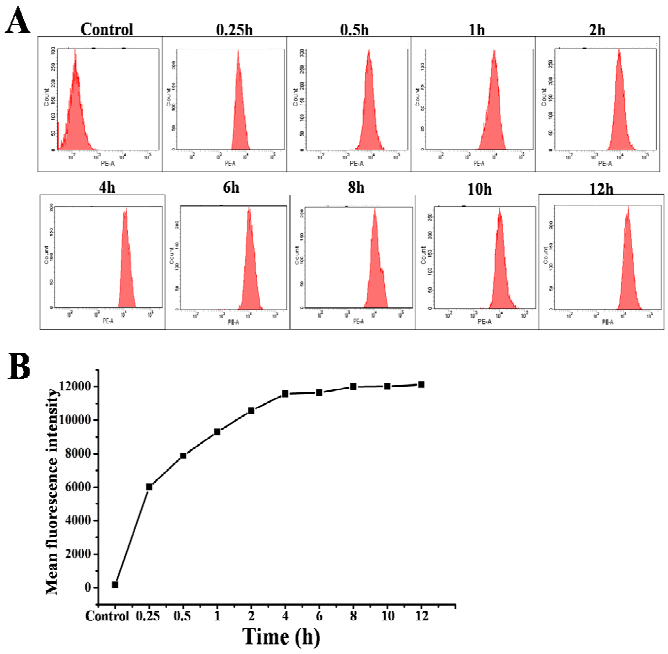

Figure 6. (A) The representative flow cytometric profiles of MCF-7 cells treated with NR-loaded HPG-2S-SN38 micelles for different time intervals. (B) The relative geometrical mean fluorescence intensities of NR-loaded HPG-2S-SN38 micelles pretreated cells.

Cell internalization

To confirm whether the CA-loaded HPG-2S-SN38 micelles could be effectively transported into tumor cells, both the flow cytometry analysis and fluorescence microscopy were performed to measure the cellular uptake of the CA-loaded HPG-2S-SN38 in MCF-7 cells. The hydrophobic NR was used as a fluorescent probe in place of CA and encapsulated into the core of HPG-2S-SN38 micelles since CA shows no obvious fluorescence. The stability of NR-loaded HPG-2S-SN38 micelles was evaluated in PBS buffer (pH 7.4) at 37 °C in the presence or absence of H_2O_2. As shown in Figure S7, NR-loaded HPG-2S-SN38 micelles release NR rapidly in the presence of H_2O_2 while minimal NR is released even after 48 h incubation in the absence of H_2O_2, suggesting the relatively high stability of NR-loaded HPG-2S-SN38 micelles under physiological condition. As displayed in Figure 6A, the flow cytometric histograms of the pretreated cells incubating with NR-loaded HPG-2S-SN38 micelles shift obviously to the direction of high fluorescence intensity in comparison with that of the control cells. The relative geometrical mean fluorescence intensities of NR-loaded micelles pretreated cells increase from 40- to 80-fold of non-pretreated cells with the incubation time from 0.25 h to 4 h while remaining almost constant after 4 h, as shown in Figure 6B. The apparent enhancement of fluorescence intensity demonstrates the effective internalization of HPG-2S-SN38 micelles.

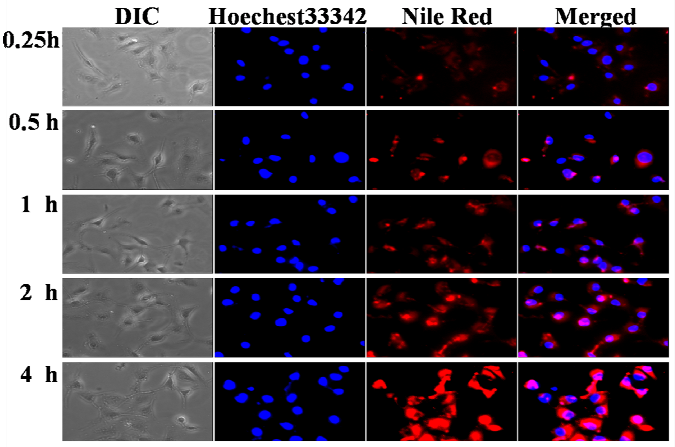

Figure 7. Fluorescence images of MCF-7 cells treated with NR-loaded HPG-2S-SN38 micelles for 0.25 h, 0.5 h, 1 h, 2 h and 4 h, respectively.

Moreover, the cellular uptake of NR-loaded HPG-2S-SN38 micelles was further investigated by fluorescence microscopy and confocal laser scanning microscopy. MCF-7 cells were treated with NR-loaded HPG-2S-SN38 micelles at 37 ºC for 0.25 h, 0.5 h, 1 h, 2 h and 4 h, respectively. The cell nucleus was stained by Hoechst33342. Figure 7 shows that the MCF-7 cells incubated for 0.25 h, 0.5 h, 1 h exhibit the red fluorescence of NR mainly in cytoplasm. The fluorescence intensity becomes stronger with increasing time. Subsequently, the MCF-7 cells show enhanced red fluorescence mainly in cytoplasm with the incubation time increases to 2 h and 4 h (Figure S8 and the video in Supplementary Information). It is further confirmed that the effective internalization of HPG-2S-SN38 micelles by cancer cells.

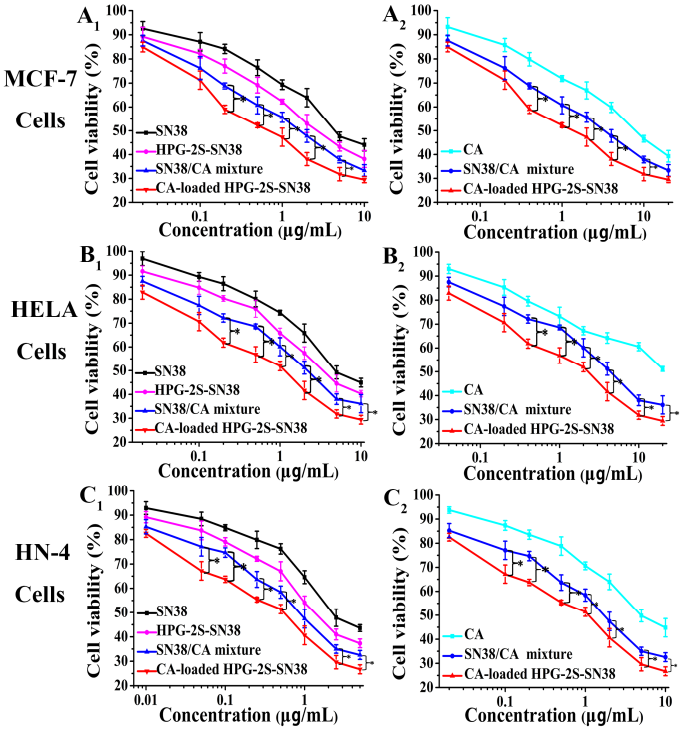

Figure 8. Cell viability of (A1, A2) MCF-7 cells, (B1, B2) HeLa cells, and (C1, C2) HN-4 cells after 48 h treated with CA, SN38, HPG-2S-SN38 micelles, the physical mixture of SN38 and CA, and the CA-loaded HPG-2S-SN38 micelles at various SN38 (A1, B1, C1) and CA (A2, B2, C2) concentrations. IC50 values are summarized in Table 2. Data are presented as average ± standard error (n = 4), and the statistical significance level is *P < 0.05.

Table 2. *In vitro* growth inhibitory activity of CA-loaded HPG-2S-SN38, SN38/CA mixture, HPG-2S-SN38, SN38 and CA to human cancer cell lines (MTT assay) (48 h treatment).

Cell line	IC_{50} (μg/mL)						
	CA-loaded HPG-2S-SN38		SN38/CA Mixture		HPG-2S-SN38	SN38	CA
	SN38	CA	SN38	CA	SN38		
MCF-7	0.68	1.40	1.58	3.34	2.61	4.35	7.94
HELA	1.14	4.25	2.17	4.25	3.31	4.87	19.8
HN-4	0.55	1.10	0.85	1.71	1.33	2.20	5.04

***In vitro* anticancer effect of CA-loaded HPG-2S-SN38 micelles**

The smart redox responsiveness and excellent cellular uptake capacity of CA-loaded HPG-2S-SN38 micelles made it significant to investigate their potential for anticancer drug delivery. Firstly, the cytotoxicity of pure HPG was evaluated by MTT assay using MCF-7 cells. Figure S9 displays the cell viability incubation with the HPG at different concentrations. No obvious cytotoxicity against tumor

cells is observed after 48 h even when the concentration of copolymer micelles is up to 2 mg/mL. Apparently, the HPG has low cytotoxicity to tumor cells. Then the anticancer activity of the CA-loaded HPG-2S-SN38 nanomicelles was investigated against MCF-7 cells, HN-4 cells and HeLa cells. As the controls, the free CA, free SN38, HPG-2S-SN38 micelles, and the physical mixture of SN38 and CA were also investigated under identical conditions. The *in vitro* cytotoxicity of all the five formulations to human cancer cell lines is shown in Figure 8 and the IC_{50} values have been summarized in Table 2. It is found that after 48 h incubation, the cytotoxicity of these formulations is concentration-dependent. Both the CA-loaded HPG-2S-SN38 nanomicelles and the physical mixture of SN38 and CA show higher anticancer activity than free SN38, free CA and HPG-2S-SN38 micelles in MCF-7 cells, HeLa cells and HN-4 cells. It is indicated that CA and SN38 have the additive or synergistic anticancer activity. Furthermore, the CA-loaded HPG-2S-SN38 nanomicelles show higher activity than the physical mixture of SN38 and CA. The reason that the CA-loaded HPG-2S-SN38 nanomicelles enhance the cytotoxicity may be attributed to the efficient intracellular uptake and endosomal escape of nanomicelles. On the other hand, the CA-loaded HPG-2S-SN38 nanomicelles enhance the solubility of hydrophobic CA and SN38 and release them in a controlled way. H_2O_2-mediated intracellular cleavage of HPG-2S-SN38 in the cancer cells results in the disassembly of the micelles and promotes the release of encapsulated CA. The preferential release of CA from CA-loaded HPG-2S-SN38 micelles leads to intracellular generation of ROS, which in turns accelerates the degradation rate of HPG-2S-SN38. Therefore, the co-delivery of CA and SN38 in nanomicelles triggers a significantly more ROS generation in the cancer cells and induced more cell death. As a control, the cytotoxicity of the CA-loaded HPG-2S-SN38 nanomicelles against normal cells (L929 cells) was also evaluated under identical conditions to make sure that H_2O_2 is the main trigger to degrade HPG-2S-SN38 to cause cell death. Indeed, it has been demonstrated that CA-loaded HPG-2S-SN38 nanomicelles exhibit a much lower cytotoxicity against normal cells than tumor cells (Figure S10).

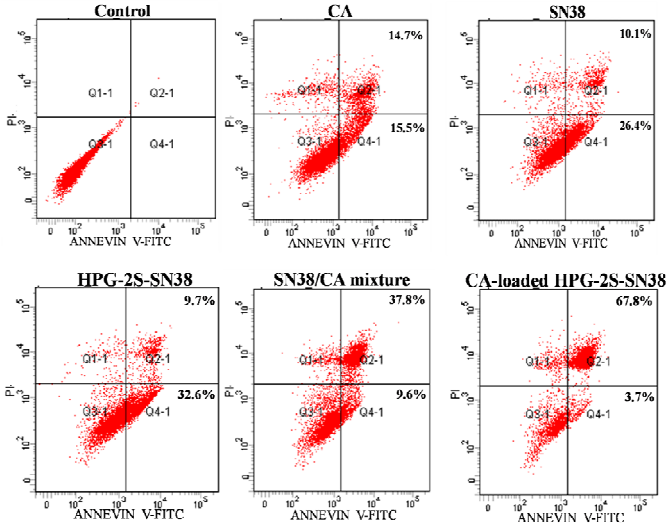

Figure 9. (A) Representative flow cytometric analysis results of cell apoptosis of MCF-7 cells treated with the CA, SN38, HPG-2S-SN38 micelles, the physical mixture of SN38 and CA, and the CA-loaded HPG-2S-SN38 micelles at the same SN38 concentrations (10 μg/mL) and CA concentrations (20 μg/mL) for 24 h. Inserted numbers in the profiles represent the percentage of the cells present in this area. Lower left, living cells; Upper left, necrotic cells; Lower right, early apoptotic cells; Upper right, late apoptotic cells.

Apoptosis-inducing effect of CA-loaded HPG-2S-SN38 micelles

To determine whether the inhibition of cancer cell proliferation by these drug-loaded micelles was a consequence of CA and SN38 induced apoptosis, we conducted the FITC-Annexin V/PI double-staining assay in MCF-7 cells. Firstly, MCF-7 cells were treated with the CA, SN38, HPG-2S-SN38 micelles, the physical mixture of SN38 and CA, and the CA-loaded HPG-2S-SN38 micelles at the same SN38 concentrations (10 μg/mL) and CA concentrations (20 μg/mL) for 24 h, and then subjected to FITC-Annexin V/PI staining. The MCF-7 cells without any treatment were set as a control. Flow cytometry data show that after treated with the CA, SN38, HPG-2S-SN38 micelles, the physical mixture of SN38 and CA, and the CA-loaded HPG-2S-SN38 micelles, the ratio of apoptotic cells in MCF-7 cells are 30.2%, 36.5%, 42.3%, 47.4% and 71.5%, respectively (Figure 9). Obviously, the CA-loaded HPG-2S-SN38 micelles induce a much higher level of apoptosis in cancer cells with the same dose, which is consistent with MTT results.

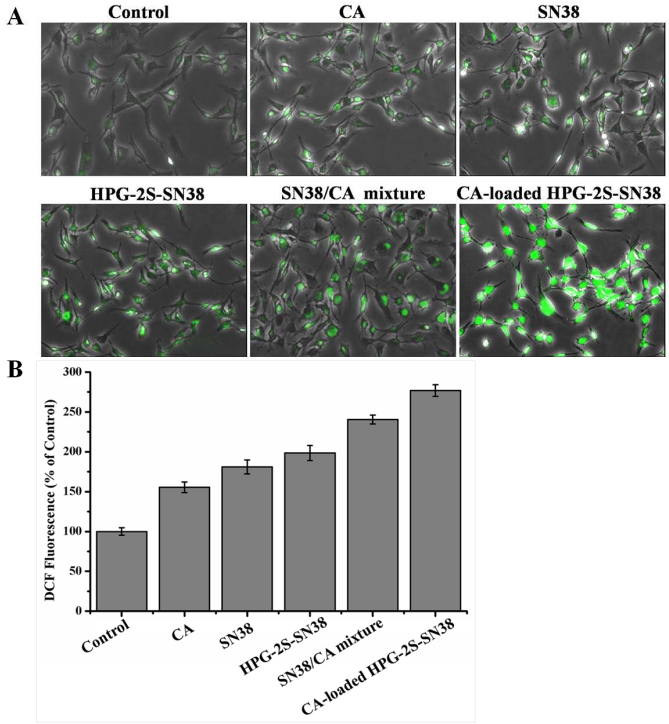

Figure 10. Generation of ROS in MCF-7 cells. (A) Representative fluorescence images of MCF-7 cells treated with CA, SN38, HPG-2S-SN38 micelles, the physical mixture of SN38 and CA, and the CA-loaded HPG-2S-SN38 nanomicelles at the same SN38 (10 μg/mL) and CA (20 μg/mL) concentrations for 24 h. (B) Relative quantification of intracellular ROS generation measured by the DCFH-DA assay after 24 h exposure to five different formulations at the same dose of CA (20 μg/mL) and SN38 (10 μg/mL). Untreated MFC-7 cells were set as a control.

Determination of intracellular ROS levels

The anticancer drugs CA and SN38 are known to induce the production of intracellular ROS that mediates cell apoptosis. Firstly, the ability of CA-loaded HPG-2S-SN38 micelles to generation of ROS was assessed by fluorescence microscopy using a selective fluorescence marker 2',7'-dichlorfluorescein-diacetate (DCFH-DA). DCFH-DA has no fluorescence, but could be activated by ROS including H_2O_2 and become fluorescent 2',7'-dichlorfluorescein (DCF).[60] Figure 10A shows the representative fluorescence images of MCF-7 treated with five different drug formulations. The cells

without any treatment were set as a control, and almost no fluorescence is observed. Cells exposed to free CA, SN38 and HPG-2S-SN38 micelles for 24 h exhibit green fluorescence, suggesting that both CA and SN38 can induce the generation of intracellular ROS, which converts non-fluorescent DCFH-DA to fluorescent DCF. The combination of CA and SN38 shows enhanced ROS generation, while treatment with CA-loaded HPG-2S-SN38 micelles induces higher ROS level in MCF-7 cells. It is suggested that CA-loaded HPG-2S-SN38 micelles can effectively deliver both CA and SN38 into cells and increase the ROS level, which is beneficial for enhanced apoptosis of tumor cells.

Furthermore, the intracellular ROS level in MCF-7 cells incubated with all these five formulations was determined by a fluorometric assay using DCF fluorescence intensity.[61] After exposed to different drug formulations for 24 h, the tumor cells were incubated with 30 μM DCFH-DA at 37 °C for 30 min. As displayed in Figure 10B, CA-loaded HPG-2S-SN38 micelles trigger a remarkably more ROS generation in the tumor cells compared to other drug formulation at the equivalent dose, which is in accordance with the results of cell apoptosis.

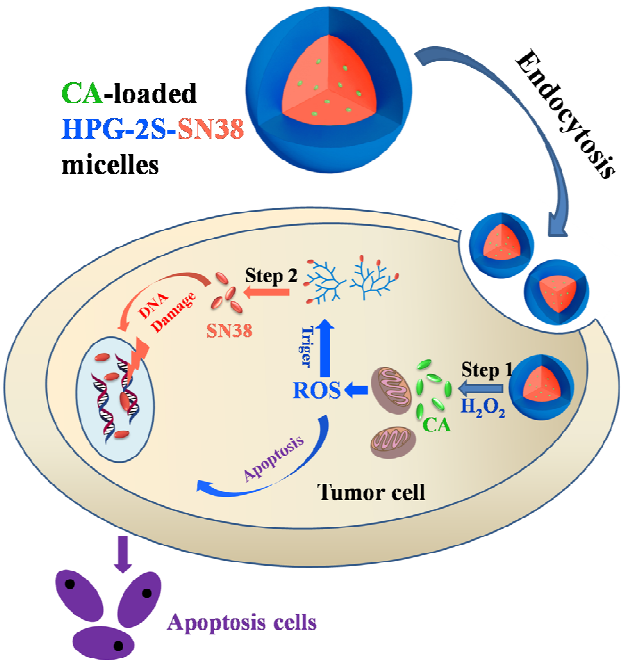

Scheme 3. Schematic representation for proposed mechanism of cell apoptosis induced by CA-loaded HPG-2S-SN38 nanomicelles. The anticancer CA-loaded HPG-2S-SN38 nanomicelles could effectively cause apoptotic cell death in tumor cells through ROS generation.

Based on the aforementioned results, we put forward the mechanism of the anticancer agent SN38 and CA into a hyperbranched polymer nano-delivery system for combination cancer treatment (Scheme 3).

Apoptosis-related protein expression regulated by CA-loaded HPG-2S-SN38 micelles

Caspase-3 plays a critical role in the execution of the apoptotic program.[62,63] The activity of caspase-3 was quantified to further evaluated the tumor cell apoptosis response to various treatments. MCF-7 cells were treated with CA, SN38, HPG-2S-SN38 micelles, the physical mixture of SN38 and CA, and the CA-loaded HPG-2S-SN38 micelles at the same dose of CA (20 μg/mL) and SN38 (10 μg/mL) for 24 h, and then the activity of caspase-3 was detected. As shown in Figure 11, when compared to control, treatment with CA, SN38, the physical mixture of SN38 and CA, or the CA-loaded HPG-2S-SN38 micelles for 24 h activates caspase-3 significantly with about 1.2-fold, 1.4-fold, 1.6-fold, 2.0-fold and 2.7-fold increase of caspase-3 activity, respectively. Obviously, the co-administration of CA and SN38 is more effective to improve the activation of caspase-3 in comparison with the single agent, and the CA-loaded HPG-2S-SN38 micelles statistically surpass other drug formulations in activating apoptosis. These data indicate that the CA-loaded HPG-2S-SN38 micelles can significantly enhance the apoptosis of MCF-7 cells.

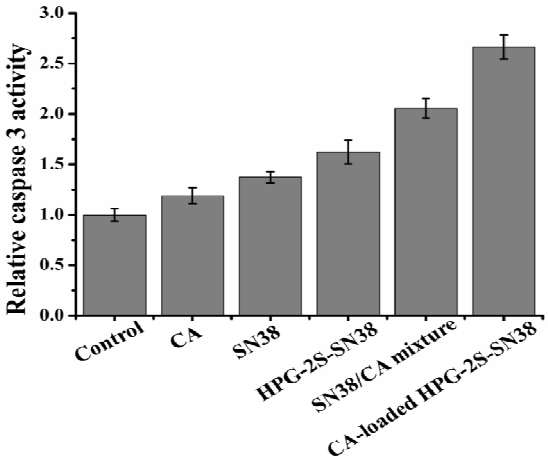

Figure 11. Activation analysis of apoptotic protein caspase-3 in MCF-7 cells. Values represent Mean ± SD.

Conclusions

A new kind of H_2O_2-responsive HPG-based nanomicelles, loaded with chemotherapy drugs SN38 and CA, was developed for effective cancer therapy through enhanced apoptotic cell death. The hyperbranched polymeric nanomicelles improve the solubility and stability of hydrophobic SN38 and CA, and show H_2O_2 concentration-dependent drug release. *In vitro* studies demonstrate that CA-loaded HPG-2S-SN38 micelles exhibit improved cell apoptosis in cancer cells through the generation of intracellular ROS and their anticancer activities are markedly enhanced when compared with CA, SN38, HPG-2S-SN38 micelles and the mixture of CA and SN38. We anticipate that H_2O_2-responsive hyperbranched polymer micelles for enhanced cell apoptosis through ROS generation hold great potential as applicable anticancer therapeutics.

Acknowledgements

This work was financially supported by the National Basic Research Program (2015CB931801), National Natural Science Foundation of China (81272466), Provincial Youth Science Fund of Heilongjiang (QC2011C037), Yu Weihan fund of Harbin Medical University, Province International Cooperation Project (WB13C101), Returned Overseas Scholars Fund in Heilongjiang (LC2009C04).

Notes and references

[a] Department of Oral and Maxillofacial Surgery, The First Affiliated Hospital of Harbin Medical University, 23 Youzheng Street, Nangang District, Harbin 150001, People's Republic of China.
Address correspondence to liguolin@126.com and flguo1967@126.com

[b] School of Chemistry and Chemical Engineering, State Key Laboratory of Metal Matrix Composites, Shanghai Jiao Tong University, 800 Dongchuan Road, Shanghai 200240, People's Republic of China. Tel.: +86-21-34203400; Fax: +86-21-54741297
[c] Department of Periodontology, The First Affiliated Hospital of Harbin Medical University, 23 Youzheng Street, Nangang District, Harbin 150001, People's Republic of China

† Electronic supplementary information (ESI) available: The ^{1}H NMR spectra and DSC curves of HPG and HPG-2S-SN38, HPLC and MS spectra of HPG-2S-SN38 micelles treated with H_2O_2, nile red release from HPG-2S-SN38 micelles, MTT of HPG.

‡ These authors are joint first authors.

1 J. Ferlay, H.-R. Shin, F. Bray, D. Forman, C. Mathersn and D. M. Parkin, *J. Cancer*, 2010, **127**, 2893-2917.
2 D. Peer, J. M. Karp, S. Hong, O. C. Farokhzad, R. Margalit and R. Langer, *Nat. Nanotechnol.*, 2007, **2**, 751-760.
3 P. Huang, D. L. Wang, Y. Su, W. Huang, Y. F. Zhou, D. X. Cui, X. Y. Zhu, and D. Y. Yan, *J. Am. Chem. Soc*., 2014, **136**, 11748-11756.
4 D. C. Han, M.-Y. Lee, K. D. Shin, S. B. Jeon, J. M. Kim, K.-H. Son, H.-C. Kim, H.-M. Kim and B.-M. Kwon, *J. Biol. Chem.*, 2004, **279**, 6911-6920.
5 S. H. Hong, J. Kim, J.-M. Kim, S.-Y. Lee, D.-S. Shin, K.-H. Son, D. C. Han, Y. K. Sung and B.-M. Kwon, *Biochem. Pharmacol.*, 2007, **74**, 557-565.
6 Y.-M. Han, D.-S. Shin, Y.-J. Lee, I. A. Ismail, S.-H. Hong, D. C. Han and B.-M. Kwon, *Bioorg. Med. Chem. Lett.*, 2011, **21**, 747-751.
7 G. T. Wondrak, *Antioxid. Redox Signal.*, 2009, **11**, 3013-3069.
8 J. M. Matés and F. M. Sánchez-Jiménez, *Int. J. Biochem. Cell Biol.*, 2000, **32**, 157-170.
9 H.-U. Simon, A. Haj-Yehia and F. Levi-Schaffer, *Apoptosis*, 2000, **5**, 415-418.
10 M. L. Circu and T. Y. Aw, *Free Radic. Biol. Med.*, 2010, **48**, 749-762.
11 P. T. Schumacker, *Cancer cell*, 2006, **10**, 175-176.
12 L. Lv, L. Zheng, D. Dong, L. Xu, L. Yin, Y. Xu, Y. Qi, X. Han and J. Peng, *Food Chem. Toxicol.*, 2013, **59**, 657-669.
13 K.-E. Hwang, C. Park, S.-J. Kwon, Y.-S. Kim, D.-S. Park, M.-K. Lee, B.-R. Kim, S.-H. Park, K.-H. Yoon and E.-T. Jeong, *Int. J. Oncol.*, 2013, **43**, 262-270.
14 K. Chandra-Kuntal, J. Lee and S. V. Singh, *Breast Cancer Res. Treat.*, 2013, **138**, 69-79.
15 C. Martin-Cordero, A. Jose Leon-Gonzalez, J. Manuel Calderon-Montano, E. Burgos-Moron and M. Lopez-Lazaro, *Curr. Drug Targets*, 2012, **13**, 1006-1028.
16 N. Azad and A. K. V. Iyer, *Systems Biology of Free Radicals and Antioxidants*, 2014, 113-135.
17 J. A. Hubbell and A. Chilkoti, *Science*, 2012, **337**, 303-305.
18 D. L. Wang, T. Y. Zhao, X. Y. Zhu, D. Y. Yan and W. X. Wang, *Chem. Soc. Rev.*, 2015, DOI: 10.1039/C4CS00229F.
19 M. Scholl, T. Q. Nguyen, B. Bruchmann and H.-A. Klok, *Macromolecules*, 2007, **40**, 5726-5734.
20 M. Calderón, M. A. Quadir, S. K. Sharma and R. Haag, *Adv. Mater.*, 2010, **22**, 190-218.
21 D. Wilms, S.-E. Stiriba and H. Frey, *Acc. Chem. Res.*, 2009, **43**, 129-141.
22 Y. H. Kim and O. W. Webster, *Polym. Prepr. (Am. Chem. Soc., Div. Polym. Chem.)*, 1988, **29**, 310-311.
23 Y. H. Kim and O. W. Webster, *J. Am. Chem. Soc*., 1990, **112**, 4592-4593.
24 D. A. Tomalia and J. M. J. Fréchet, *J. Polym. Sci., Part A: Polym. Chem.*, 2002, **40**, 2719-2728.
25 A. Carlmark, C. Hawker, A. Hult and M. Malkoch, *Chem. Soc. Rev.*, 2009, **38**, 352-362.
26 S. Peleshanko and V. V. Tsukruk, *Prog. Polym. Sci.*, 2008, **33**, 523-580.
27 M. Jikei and M. Kakimoto, *Prog. Polym. Sci.*, 2001, **26**, 1233-1285.
28 A. Sunder, R. Hanselmann, H. Frey and R. Mülhaupt, *Macromolecules*, 1999, **32**, 4240-4246.
29 M. Calderon, R. Graeser, F. Kratz and R. Haag, *Bioorg. Med. Chem. Lett.*, 2009, **19**, 3725-3728.
30 D. Groger, M. Kerschnitzki, M. Weinhart, S. Reimann, T. Schneider, B. Kohl, W. Wagermaier, G. Schulze-Tanzil, P. Fratzl and R. Haag, *Adv. Healthcare Mater.*, 2014, **3**, 375-385.
31 V. M. Garamus, T. V. Maksimova, H. Kautz, E. Barriau, H. Frey, U. Schlotterbeck, S. Mecking and W. Richtering, *Macromolecules*, 2004, **37**, 8394-8399.
32 D. Wilms, F. Wurm, J. R. Nieberle, P. Böhm, U. Kemmer-Jonas and H. Frey, *Macromolecules*, 2009, **42**, 3230-3236.
33 C. Gao and D. Y. Yan, *Prog. Polym. Sci.*, 2004, **29**, 183-275.
34 B. I. Voit and A. Lederer, *Chem. Rev.*, 2009, **109**, 5924-5973.
35 T. Zhao, H. Zhang, B. Newland, A. Aied, D. Zhou and W. Wang, *Angew. Chem., Int. Ed.*, 2014, **53**, 6095-6100.
36 T. Zhao, Y. Zheng, J. Poly and W. Wang, *Nat. Commun.* 2013, **4**, 1873.
37 W. Wang, Y. Zheng, E. Roberts, C. J. Duxbury, L. Ding, D. J. Irvine and S. M. Howdle, *Macromolecules*, 2007, **40**, 7184-7194.
38 Y. F. Zhou, W. Huang, J. Y. Liu, X. Y. Zhu and D. Y. Yan, *Adv. Mater.*, 2010, **22**, 4567-4590.
39 J. Y. Liu, W. Huang, Y. Pang, P. Huang, X. Y. Zhu, Y. F. Zhou and D. Y. Yan, *Angew. Chem., Int. Ed.*, 2011, **123**, 9328-9332.
40 D. L. Wang, H. Y. Chen, Y. Su, F. Qiu, L. J. Zhu, X. Y. Huan, B. S. Zhu, D. Y. Yan, F. L. Guo and X. Y. Zhu, *Polym. Chem.*, 2013, **4**, 85-94.
41 D. L. Wang, G. S. Tong, R. J. Dong, Y. F. Zhou, J. Shen and X. Y. Zhu, *Chem. Commun.*, 2014, **50**, 11994-12017.
42 W. Saiyin, D. L. Wang, L. L. Li, L. J. Zhu, B. Liu, L. J. Sheng, Y. W. Li, B. S. Zhu, L. M. Mao, G. L. Li and X. Y. Zhu, *Mol. Pharm.*, 2014, **11**, 1662-1675.
43 R. J. Dong, Y. Liu, Y. F. Zhou, D. Y. Yan and X. Y. Zhu, *Polym. Chem.*, 2011, **2**, 2771-2774.
44 Y. Pang, J. Y. Liu, Y. Su, B. S. Zhu, W. Huang, Y. F. Zhou, X. Y. Zhu and D. Y. Yan, *Sci. China Chem.*, 2010, **53**, 2497-2508.
45 F. Qiu, D. L. Wang, Q. Zhu, L. J. Zhu, G. S. Tong, Y. F. Lu, D. Y. Yan and X. Y. Zhu, *Biomacromolecules*, 2014, **15**, 1355-1364.
46 J. Y. Liu, Y. Pang, W. Huang, Z. Y. Zhu, X. Y. Zhu, Y. F. Zhou and D. Y. Yan, *Biomacromolecules*, 2011, **12**, 2407-2415.
47 J. Y. Liu, Y. Pang, Z. Y. Zhu, D. L. Wang, C. T. Li, W. Huang, X. Y. Zhu and D. Y. Yan, *Biomacromolecules*, 2013, **14**, 1627-1636.
48 S. D. Lim, C. Sun, J. D. Lambeth, F. Marshall, M. Amin, L. Chung, J. A. Petros and R. S. Arnold, *Prostate*, 2005, **62**, 200-207.

49 M. Zieba, M. Suwalski, S. Kwiatkowska, G. Piasecka, I. Grzelewska-Rzymowska, R. Stolarek and D. Nowak, *Respir. Med.*, 2000, **94**, 800-805.
50 R. J. Dong, L. Z. Zhou, J. L. Wu, C. L. Tu, Y. Su, B. S. Zhu, H. C. Gu, D. Y. Yan and X. Y. Zhu, *Chem. Commun.*, 2011, **47**, 5473-5475.
51 Y. Pommier, *Nat. Rev. Cancer*, 2006, **6**, 789-802.
52 J. Wang, X. Sun, W. Mao, W. Sun, J. Tang, M. Sui, Y. Shen and Z. Gu, *Adv. Mater.*, 2013, **25**, 3670-3676.
53 J. A. Zhang, T. Xuan, M. Parmar, L. Ma, S. Ugwu, S. Ali and I. Ahmad, *Int. J. Pharm.*, 2004, **270**, 93-107.
54 A. Napoli, M. Valentini, N. Tirelli, M. Müller and J. A. Hubbell, *Nat. Mater.*, 2004, **3**, 183-189.
55 D. L. Wang, Y. Su, C. Y. Jin, B. S. Zhu, Y. Pang, L. J. Zhu, J. Y. Liu, C. L. Tu, D. Y. Yan and X. Y. Zhu, *Biomacromolecules*, 2011, **12**, 1370-1379.
56 V. Istratov, H. Kautz, Y.-K. Kim, R. Schubert and H. Frey, *Tetrahedron*, 2003, **59**, 4017-4024.
57 B. Kim, E. Lee, Y. Kim, S. Park, G. Khang and D. Lee, *Adv. Funct. Mater.*, 2013, **23**, 5091-5097.
58 H. Ka, H.-J. Park, H.-J. Jung, J.-W. Choi, K.-S. Cho, J. Ha and K.-T. Lee, *Cancer Lett.*, 2003, **196**, 143-152.
59 K. Lee, B.-M. Kwon, K. Kim, J. Ryu, S. J. Oh, K. S. Lee, M.-G. Kwon, S.-K. Park, J. S. Kang and C. W. Lee, *Xenobiotica*, 2009, **39**, 255-265.
60 S. Kim, H. Park, Y. Song, D. Hong, O. Kim, E. Jo, G. Khang and D. Lee, *Biomaterials*, 2011, **32**, 3021-3029.
61 Y. Bo, C. Y. Jin, Y. Liu, W. Yu and H. Kang, *Toxicol. Mech. Method.* 2014, **24**, 461-469.
62 A. G. Porter and R. U. Jänicke, *Cell Death Differ.*, 1999, **6**, 99-104.
63 K. Friedrich, T. Wieder, C. Von Haefen, S. Radetzki, R. Jänicke, K. Schulze-Osthoff, B. Dörken and P. T. Daniel, *Oncogene*, 2001, **20**, 2749-2760.

A Table of Contents Entry

Hydrogen peroxide-responsive anticancer hyperbranched polymer micelles for enhanced cell apoptosis

Bing Liu, Dali Wang, Yakun Liu, Qian Zhang, Lili Meng, Huirong Chi, Jinna Shi, Guolin Li, Jichen Li and Xinyuan Zhu

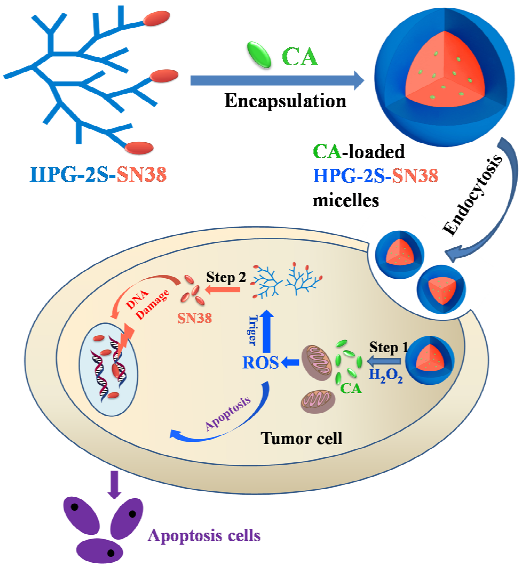

Hydrogen peroxide-responsive nanomicelles from hyperbranched polymer were developed for effective cancer therapy through enhanced apoptotic cell death.